Monthly Notices
of the
ROYAL ASTRONOMICAL SOCIETY

Mon. Not. R. Astron. Soc. **424,** 2943–2953 (2012) doi:10.1111/j.1365-2966.2012.21436.x

Principal component analysis of background and sunspot magnetic field variations during solar cycles 21–23

V. V. Zharkova,[1⋆] S. J. Shepherd[2] and S. I. Zharkov[3]

[1]*Department of Mathematics, School of Computing, Informatics and Media, University of Bradford, Bradford BD7 1DP*
[2]*Department of Mathematics, School of Engineering, Design and Technology, University of Bradford, Bradford BD7 1DP*
[3]*Mullard Space Science Laboratory, University College London, Holmbury St Mary, Dorking RH5 6NT*

Accepted 2012 May 29. Received 2012 May 14; in original form 2012 April 5

ABSTRACT

The aim of this paper is to derive the principal components (PCs) in variations of (i) the solar background magnetic field (SBMF), measured by the Wilcox Solar Observatory with low spatial resolution for solar cycles 21–23, and (ii) the sunspot magnetic field (SMF) in cycle 23, obtained by SOHO/MDI. For reduction of the component dimensions, principal component analysis (PCA) is carried out to identify global patterns in the data and to detect pairs of PCs and corresponding empirical orthogonal functions (EOFs). PCA reveals two main temporal PCs in the SBMF of opposite polarities originating in opposite hemispheres and running noticeably off-phase (with a delay of about 2.5 yr), with their maxima overlapping in the most active hemisphere for a given cycle. Their maximum magnitudes are reduced by a factor of 3 from cycle 21 to 23, and overlap in the Northern hemisphere for cycle 21, in the Southern one in cycle 22 and in the Northern one again in cycle 23. The reduction of magnitudes and slopes of the maxima of the SBMF waves from cycle 21 to cycle 23 leads us to expect lower magnitudes of the SBMF wave in cycle 24. In addition, PCA allowed us to detect four pairs of EOFs in the SBMF latitudinal components: the two main latitudinal EOFs attributed to symmetric types and another three pairs of EOFs assigned to asymmetric types of meridional flows. The results allow us to postulate the existence of dipole and quadruple (or triple-dipole) magnetic structures in the SBMF, which vary from cycle to cycle and take the form of two waves travelling off-phase, with a phase shift of one-quarter of the 11 yr period. Similar PC and EOF components were found in temporal and latitudinal distributions of the SMF for cycle 23, revealing polarities opposite to the SBMF polarities, and a double maximum in time or maxima in latitude corresponding to the maxima of the SBMF PC residuals or minima in the SBMF EOFs, respectively. This suggests that the SBMF waves modulate the occurrence and magnitude of the SMF in time and latitude.

Key words: Sun: activity – Sun: magnetic topology – sunspots.

1 INTRODUCTION

Solar activity is assumed to be generated by magnetic dynamo waves of poloidal field travelling from one pole to the other during an 11-yr cycle (or 22 yr for the full magnetic polarity change), while producing strong (toroidal) magnetic fields seen as sunspots (Parker 1955). There are two major factors considered to affect their interaction: the α and Ω effects, where Ω is an angular velocity and α is a factor linked to the mean kinetic helicity of turbulent motion (Steenbeck, Krause & Rädler 1966).

The Ω effect is associated with a radial gradient of rotation rate, allowing the flux tubes with a strong toroidal magnetic field, or sunspots, formed in the solar convective zone (SCZ) to travel towards the solar surface. Then, because of the turbulent motion occurring during the flux tube migration to the solar surface, the α effect takes over and becomes responsible for the regeneration of the poloidal (background) magnetic field from the toroidal field via a mean kinetic helicity ($v \bigtriangledown v$) of turbulent motion (Krause & Raedler 1980). Dynamo models considering the meridional circulation of magnetic fields show it to be the crucial component in defining the dynamo period and the cycle power and length (Dikpati & Gilman 2008).

Hence, a consistent relationship between these two fields throughout the whole solar cycle is still not clear, either theoretically

⋆E-mail: v.v.zharkova@bradford.ac.uk

or observationally. Schlichenmaier & Stix (1995) investigated theoretically the phase shift between the toroidal and poloidal magnetic fields for α–Ω dynamo models and found them to be in antiphase with a period of 11 yr. This was recently confirmed by simultaneous observations of the background and sunspot magnetic fields by Zharkov, Gavryuseva & Zharkova (2008), who also detected a second oscillation period of about 2.5 yr during which the background magnetic field is subject of imposed oscillations of lower magnitude. This component has opposite signs in each hemisphere, coinciding with, or opposing, the leading polarity of sunspots. It changes its sign every 2.5 yr, causing an excess (when opposing) or deficit (when coinciding with the leading sunspot polarity) in the number of sunspots appearing on the solar surfaces in opposite hemispheres. This is seen as a strong north–south asymmetry in sunspot areas covered in each hemisphere and in the resulting magnetic fields contained inside sunspots.

Recent helioseismic observations of the solar differential rotation have revealed a significant radial gradient $\partial\Omega/\partial r$ around the SCZ and a latitudinal gradient of the angular velocity $\partial\Omega/\partial\theta$ near the solar surface (Schou et al. 1998). These observations have been utilized in dynamo models exploiting these two periods ($\sim$2.5 and 11 yr) of solar activity caused by the dynamo mechanisms: the lower-frequency one (11 yr) operates at the base of the SCZ because of the large-scale radial shear; and the higher-frequency one is generated in the subsurface regions by the latitudinal shear (Benevolenskaya 1998, 2003). The two-level model gives a plausible explanation of the temporal appearance of solar activity with two basic periods, namely the lower ($\sim$11 yr) and higher ($\sim$2.5 yr) frequency also reported from the statistical analysis of magnetic field observations (Zharkov et al. 2008). However, the interaction between the two types of shears and the distribution in latitude between the background (poloidal) and sunspot (toroidal) magnetic fields are still not fully understood.

Observational estimations of meridional flows defining $\partial\Omega/\partial\theta$ near the solar surface averaged over a solar cycle in the photosphere and beneath reveal significant discrepancies in the meridional shifts at different depths of the interior that are especially important for the latitudes of sunspot formation (Dikpati, Gilman & Ulrich 2010). Different methods use different properties of the measured signals, for example tracking the surface magnetic features in cycles 22 and 23 (Snodgrass & Dailey 1996; Hathaway & Rightmire 2011), or measuring Doppler signals from supergranulation in cycle 23 (Švanda, Klvaňa & Sobotka 2006), or measuring Doppler shifts of acoustic frequencies measured in cycle 23 by helioseismic methods (Basu & Antia 2006; Gizon, Birch & Spruit 2010). While the surface Doppler velocities peak at about 20° Švanda et al. (2006), the helioseismic meridional shifts peak at 30° (Basu & Antia 2006; Gizon et al. 2010); they have similar magnitudes and are broad.

The magnetic feature shifts are shown to be strongest at latitudes of about 50° (Snodgrass & Dailey 1996; Hathaway & Rightmire 2011), with the peak being about 30 per cent lower than for the other two. This location coincides nicely with the latitude of maximum tilts and charge separation in sunspot groups (Zharkova & Zharkov 2008), which can be explained by the presence of strong surface magnetic diffusion at these locations, as pointed out by Dikpati et al. (2010). Similar discrepancies in meridional flow measurements have been reported for cycle 22 (Ulrich 1993; Snodgrass & Dailey 1996; Cameron & Hopkins 1998). These observations emphasize the importance of understanding the structure of the solar background magnetic field defining these meridional motions of active solar structures on and beneath the surface (sunspots and active regions) that carry strong toroidal magnetic fields.

This implies that solar dynamo waves can have a much more complicated structure than the two simple waves assumed by the simple dynamo models, which are generated by a magnetic dipole operating at the bottom of the SCZ. Rather, they can be affected by other (unknown or not yet considered) processes, which need to be discovered and investigated. Given the complexity of variations of solar activity in each solar cycle, possible methods of such deeper investigation of solar activity have to be associated with more accurate mathematical methods of statistical analysis of solar activity developed in the past decades, such as principal component analysis (PCA). PCA allows us to search for orthogonal modes of the two-point correlation matrix constructed from a data set and permits the identification of structures that remain coherent and linearly correlated or that recur throughout a time series.

These modes, or empirical orthogonal functions (EOFs), can then be ordered according to the degree of linear correlation with the whole data set. The first benefit of this procedure is that it may allow a summary or the capture of the essential nature of the data set using a significantly reduced subset. The second benefit is that the procedure will lead to EOFs that are amenable to physical interpretation, while at the same time extracting some hidden meaning from the data. It is assumed that the EOFs may be eigenmodes of underlying physical processes that are yet to be discovered or identified.

Lawrence et al. (2004) applied PCA to the large-scale, axisymmetric magnetic field measured during one solar rotation and related this field to the solar dynamo. The authors found common periodicities between temporal variations of this magnetic field and characteristic periodicities in the solar wind and interplanetary magnetic field (IMF) (Cadavid et al. 2005a,b), and compared longitudinal variations in two different, but physically related, data sets, namely the (IMF) polarity at 1 au, and the 3.25R source-surface fields in the solar corona derived from magnetic images of the Sun in cycles 21–23 (Cadavid, Lawrence & Ruzmaikin 2008). In both data sets the authors also found close independent modes with high eigenvalues, which demonstrates their close physical connection.

With these encouraging achievements in mind, in the present paper we continue the investigation of the relationship between the solar background and sunspot magnetic fields started in our previous papers (Zharkov et al. 2008; Zharkova & Zharkov 2010), in order to derive the eigenfunctions of all the periodicities observed in both data sets and to establish the links between these fields at various latitudes during different solar cycles. This will allow us to understand the physical nature of this relationship and, possibly, link the fields to the levels in the solar interior where the solar dynamo operates.

The data used in this investigation are described in Section 2, the methods used are described in Section 3.1, the analysis of the SBMF is presented in Section 3 and that of the SMF in Section 4, with the conclusions drawn in Section 5.

2 DATA DESCRIPTION

2.1 Wilcox Solar Observatory (WSO) data

To investigate large-scale solar background magnetic field (SBMF) variations, we used low-resolution magnetograms obtained daily with the WSO Babcock solar magnetograph from the Zeeman splitting of the 525.02-nm Fe I spectral line (Hoeksema 1984). The observations of the SBMF were carried out from the beginning of Carrington rotation (CR) 1642 up to 2027 (or year 2005.16); that is, the data cover solar activity cycles 21, 22 and 23 (Scherrer et al.

1977; Hoeksema 1985). For the purpose of the present study, we consider the averaged magnetic field in cycles 21–23 within the 30 μ-hemispheres in the heliographic latitude sines (from 75°.2 north to 75°.2 south) and within 5° in heliographic longitude (around the central meridian).

2.2 Solar Feature Catalogues for sunspots

The searchable Solar Feature Catalogues (SFCs) with 12 yr coverage (1996–2008) were developed from digitized solar images using automated pattern recognition techniques (Zharkova et al. 2005). Features recognized include sunspots, active regions, filaments and line-of-sight magnetic neutral lines in automatically standardized full-disc solar images in Ca II K1, Ca II K3 and Hα lines taken at the Paris–Meudon Observatory and in white-light images and magnetograms from SOHO/MDI. The results of the automated recognition were verified with the NOAA and Meudon synoptic maps and statistical data, revealing a high detection accuracy of up to 96 per cent for sunspots (Zharkov, Zharkova & Ipson 2005) and of up to 92 per cent for active regions (Benkhalil et al. 2006).

The sunspots were extracted from the SOHO/MDI images using the automated edge-detecting technique and verified by the presence of a strong magnetic field (Zharkov et al. 2005). The parameters extracted include heliographic area, heliographic diameter, number of umbrae, Carrington and planar coordinates of the sunspot centre of gravity, maximum magnetic field, minimum field, excess flux, total (absolute) flux, maximum umbra field, minimum umbra field, excess umbra flux, total (absolute) umbra flux, the pixel and planar coordinates of the bounding rectangle, its raster scan marking the penumbral and umbral pixels, and various observational parameters entered into a relational data base of SFCs on the web site http://solar.inf.brad.ac.uk/.

For the purpose of the present study we use the absolute magnetic field confined by the areas of sunspots for both leading and trailing polarities at a given latitude and time.

3 PCA OF THE SOLAR BACKGROUND MAGNETIC FIELD

3.1 PCA method

The sunspot magnetic field (SMF) and background magnetic field at given latitudes are affected by various processes (dynamo waves, meridional flows, torsional oscillations etc.). In order to derive the main periods present in the observational data of solar activity, namely in sunspot areas, we apply PCA to derive the dominant eigenfunctions from the data and to compare them with those derived earlier.

PCA is an orthogonal linear transformation allowing a vector space to be transformed to a new coordinate system, reducing the multidimensional data to lower dimensions for analysis, so that the greatest variance by any projection of the data lies on the first coordinate, called the principal component (Pearson 1901; Jolliffe 2002).

The inner (respectively, outer) principal components of a data set represented by an $(m \times n)$ matrix $\mathbf{X}$, or the so-called principal components (PCs), are computed by projecting the original data $\mathbf{X}$ into the eigenspace of the data covariance matrices (Jolliffe 2002). Letting the desired projection be $\mathbf{Y}$, we have $\mathbf{Y} = \mathbf{XE}$ for the inner product and $\mathbf{Y} = \mathbf{EX}$ for the outer product, where $\mathbf{\Sigma} = \mathbf{S}^{\top} \cdot \mathbf{S}$ for the inner product and $\mathbf{\Sigma} = \mathbf{S} \cdot \mathbf{S}^{\top}$ for the outer product, and where $\mathbf{\Sigma}$ can be written in the canonical decomposition as follows:

$$\mathbf{\Sigma} = \mathbf{E} \cdot \mathbf{\Lambda} \cdot \mathbf{E}^{-1} \quad (1)$$

The PCs (of the data set variations in time) are those vectors of $\mathbf{Y}$ associated with the largest eigenvalues of $\mathbf{\Sigma}$. In practice, we sort the diagonal of $\mathbf{\Lambda}$ (the eigenvalues of $\mathbf{\Sigma}$) in a descending order of magnitude, together with the corresponding rows (or columns for the outer PC) of $\mathbf{E}$ (the eigenvectors of $\mathbf{\Sigma}$).

One then seeks a set of empirical orthogonal functions (EOFs) of latitude that are ordered by their correlation with the whole data set through time. The first EOF is constructed to be maximally correlated. The second EOF is also constructed to be maximally correlated, but is constrained to be orthogonal to the first EOF, and so on. The degree of correlation of each EOF with the whole data set is its eigenvalue. The projection of each EOF onto the data gives a function of time (the principal component), which indicates the importance of the corresponding of EOF at different times.

For most data sets arising from naturally observed phenomena where the data are noisy, there are comparatively few dominant eigenvalues, which represent the real signal in the data. The rest of the smaller eigenvalues represent noise, and the vectors can be discarded. Thus, this technique simultaneously (i) reduces the data dimensionality, (ii) separates the signals from noise, and (iii) orthogonalizes the resulting components so that they can be ascribed to distinct physical processes.

3.2 SBMF variations in cycles 21–23

3.2.1 Overview of the PCs derived from the SBMF

The PCA of the data set with the SBMF described in Section 2.1 allowed us to derive more than 20 eigenvalues (see Fig. 1) defining the PCs, with eight of them exceeding the 5 per cent variance level. The two largest eigenvalues are found to be responsible for 19 per cent each of the total variance of the temporal SBMF from the whole solar disc comprising 30 bands of latitude (15 in each hemisphere).

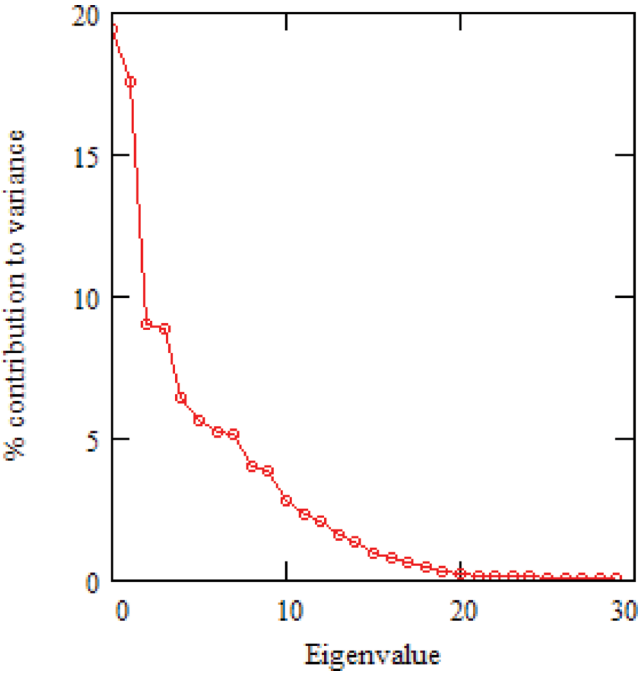

Figure 1. Leading eigenvalues of the PCA decomposition as percentage contributions of the SBMF variations over the solar cycles 21–23.

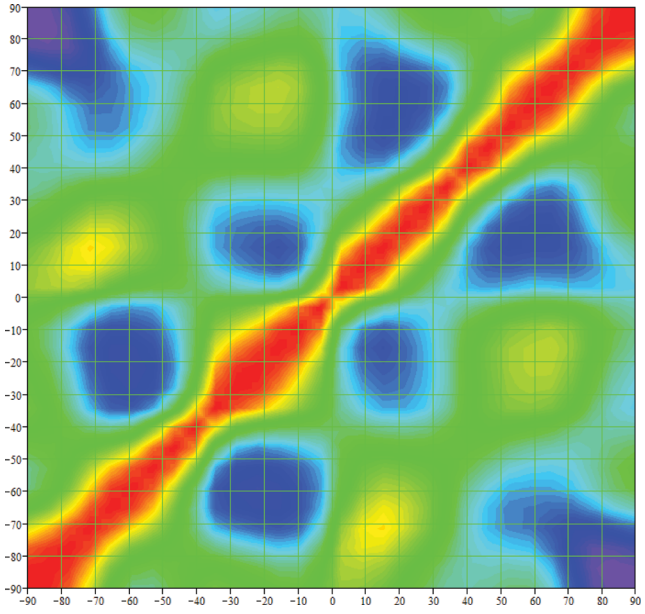

Figure 2. Auto-correlation of the data set of the SBMF in the 30 latitude bands over the whole set of solar cycles 21–23.

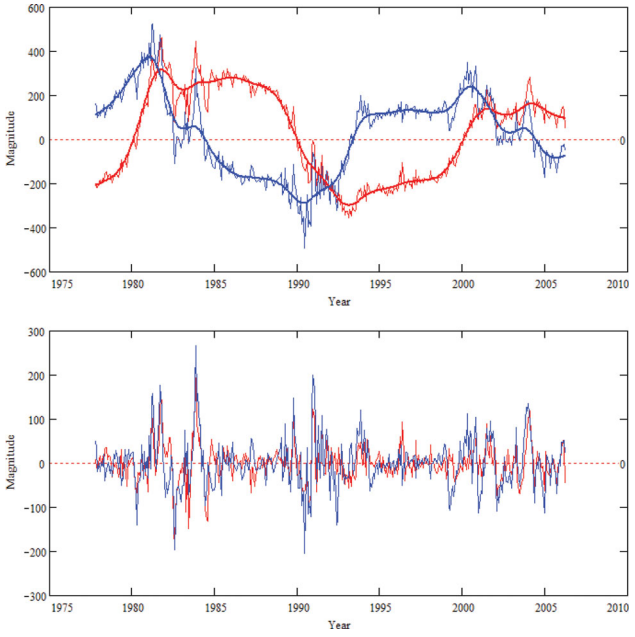

Figure 3. Upper plot: first two PCs of the SBMF distribution in latitude plotted versus time for cycles 21–23; bottom plot: their cyclic residuals from means for the two PCs above, marked by the same colour.

The eigenvalues seem to be paired into two independent components, with the two largest pairs covering 38 per cent (components 1 and 2) and 19 per cent (components 3 and 4), and three less pronounced pairs covering 13 per cent (5 and 6), 10 per cent (7 and 8) and 8 per cent (9 and 10).

It is also possible to look at the correlation of the PCs for different latitudes, plotted in Fig. 2. The correlation clearly shows the main dipoles located at the poles and two other dipoles – one located on the equatorial plane (similar to in Cadavid et al. 2008) and the other located at latitudes above $\pm 40^\circ$ – which have smaller magnitudes than the polar ones. This indicates that in this respect, the classic assumption about the single dipole magnetic field of the Sun forming the solar dynamo needs to undergo some revision.

3.2.2 Temporal variations of principal SBMF components

We carried out a PCA of the detected pairs and found that each of them are, in fact, independent components varying in time and in latitude (discussed in Section 3.3). In this section, similar to the analysis in fig. 7 in Cadavid et al. (2008), we consider the two main PC variations in time defined by the two dominant eigenvalues (latitudes exceeding any other by an order of magnitude). However, unlike Cadavid et al. (2008), we detect the pair (not three) of the most significant independent components of the SBMF with their temporal evolution shown in Fig. 3 (upper plot) and the cyclic residuals of these two components shown in Fig. 3 (lower plot).

These two main temporal PCs are found to vary strongly from cycle to cycle following the spherical harmonics of the Bessel function $Y_n^m(\theta, \phi)$, roughly resembling sine ($n = 1$ and $m = 1$) and cosine ($n = 1$, $m = 0$) functions with a period of about 10 yr (Cadavid et al. 2008). At the solar minimum, each of the waves starts from a different hemisphere where the background magnetic field has opposite polarities but travels to the same hemisphere.

This implies that these two waves have opposite magnetic polarities. One of the PCs supposedly following a cosine starts in cycle 21 with a negative polarity and crosses zeros in the years 1980, 1990 and 2000, confirming previous findings (Cadavid et al. 2008). The second PC (supposedly sine) starts in cycle 21 with a positive polarity at some phase ahead of the cosine function, which we discuss below.

Both waves continue to travel into the hemisphere, which later becomes the dominant one for the given cycle, for example to the Northern hemisphere in cycles 21 and 23 and to the Southern one in cycle 22 (see Fig. 3). The sine wave [with the negative (Southern) magnetic field magnitude] travels slightly out of phase with the cosine wave having a positive (Northern) magnetic field magnitude. Comparison of the wave phases allows us to establish that the sine wave travels ahead of the cosine wave with a shift in phase of about 90°, or 2.5 yr, which is the same magnitude as derived by Cadavid et al. (2008). As a result of this phase shift, the two temporal SBMF waves defined by the two PCs reach maximum magnitudes at different times, while approaching the same magnitude somewhere between their maxima.

Furthermore, the magnitudes of the maxima reached by each of the waves are noticeably different. This results in a double maximum in the SBMF for each given cycle, defining the double solar activity maxima first reported by Gnevyshev & Ol (1987) that are confirmed for each solar cycle. Interestingly, the cyclic residuals reveal strong fluctuations about these maxima at nearly equal temporal intervals before and after the times when the waves reach the same magnitudes. This can be interpreted as a possible resonant interaction of these two waves when the magnitudes are comparable, preceded and succeeded by the increased turbulence induced by these waves before and after the resonance period.

After the maximum, the two waves have different temporal patterns. In the odd cycles (21 and 23) the magnitude of the wave with the positive polarity (cosine) drops very steeply in the Northern hemisphere towards the equator and then moves smoothly in the Southern hemisphere. Then in the even cycle 22 it repeats its motion in the Southern hemisphere in the opposite direction: from the South to the equator and back to the North. In contrast, the wave with the negative polarity (sine) has a much smoother decrease in magnitude, staying in the Northern hemisphere in cycles 21 and 23

until approaching the solar minimum and beyond, and then moving to the Southern hemisphere in cycle 22, mirroring the pattern of the previous cycle but with opposite signs.

Again in cycle 22 both waves reach their maxima with a phase difference of about 2.5 yr, with the magnitude of the positive-polarity wave being slightly higher than that of the negative one. At certain times before and after the two waves reach the same magnitude, there are strong increases in their cyclic residuals that could be a reflection of some turbulent processes accompanying the wave interaction in the given hemisphere. The crossings of the equator occur at even periods of about 10 yr (1980, 1990 and 2000), which were the periods of solar activity maxima in cycles 21–23.

Furthermore, it can be clearly noted that the magnitudes of the maxima of the positive and negative waves steadily decrease by about 50 per cent from cycle 21 to cycle 22 and further by 50 per cent to cycle 23, approaching in the cycle 23 half of their magnitude in cycle 21. Moreover, the magnitudes where these waves intercept, or have the same magnitudes, is reduced by 30 per cent from cycle 21 to 22 and then by 50 per cent from cycle 22 to cycle 23. For example, in cycle 23, the two waves intercept at the lowest magnitude of about 100 compared with the magnitude of 300 for cycle 21 and of 200 for cycle 22. If the decrease follows the same pattern then the waves will intercept at a magnitude of about 50 in cycle 24, meaning much lower solar activity compared even to cycle 23.

3.3 Latitudinal variations of the SBMF

In order to understand the temporal variations of the PCs of the SBMF, it is necessary to investigate the latitudinal distribution of the SBMF in more detail. For this purpose we carried out a PCA of the SBMF data in 30 latitude bands for the whole set of 21–23 cycles, plotted in Fig. 4, and obtained four pairs of EOFs, plotted in

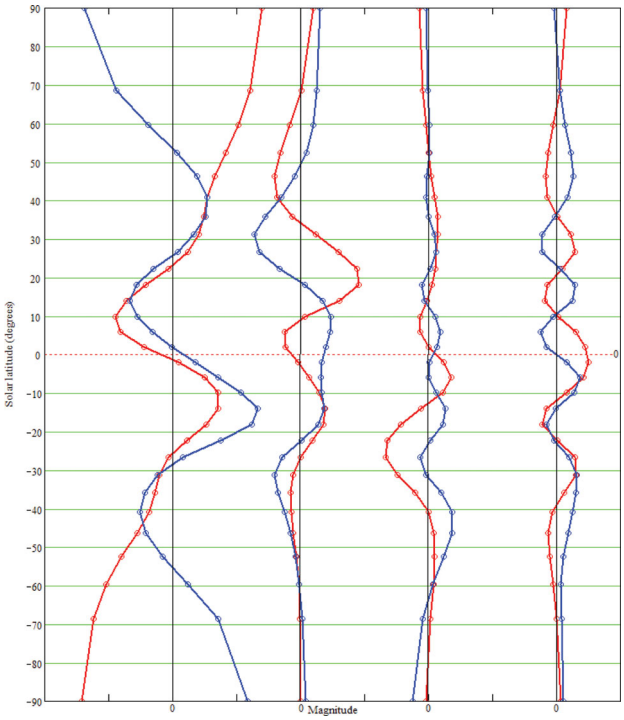

Figure 4. The eight EOFs of the SBMF over the 30 latitude bands corresponding to the common symmetric flows for all three cycles (leftmost plots), and to cycles 21 (second left plots), 22 (third left plots) and 23 (rightmost plots).

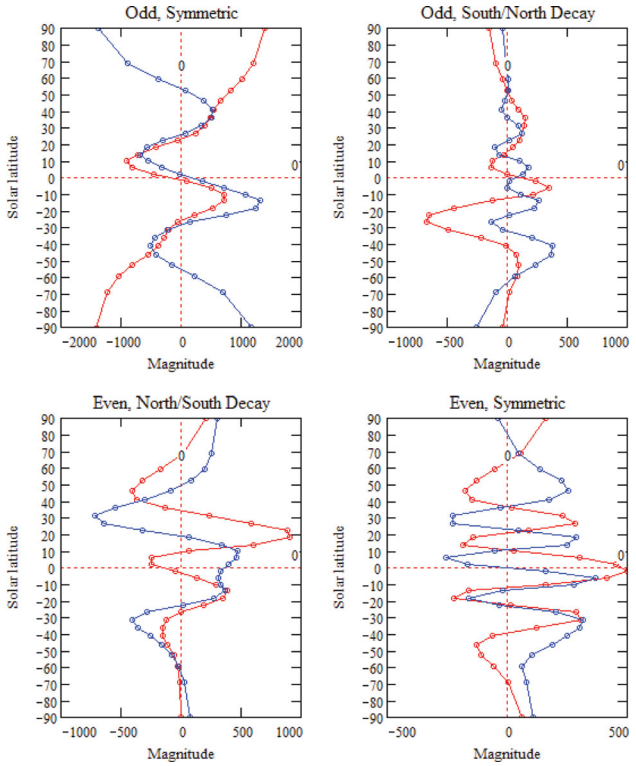

Figure 5. The eight EOFs of the SBMF plotted over the 30 latitude bands corresponding to the common symmetric flows for all three cycles (top left plot) and to the symmetric or asymmetric ones derived for cycles 21 (top right plot), 22 (bottom left plot) and 23 (bottom right plot).

Fig. 5. The cross-correlation plots between each pair of these four EOFs are shown in Fig. 6.

The two strongest EOFs, plotted in the left plot of Fig. 4, are the same for all three cycles and correspond to the same two largest

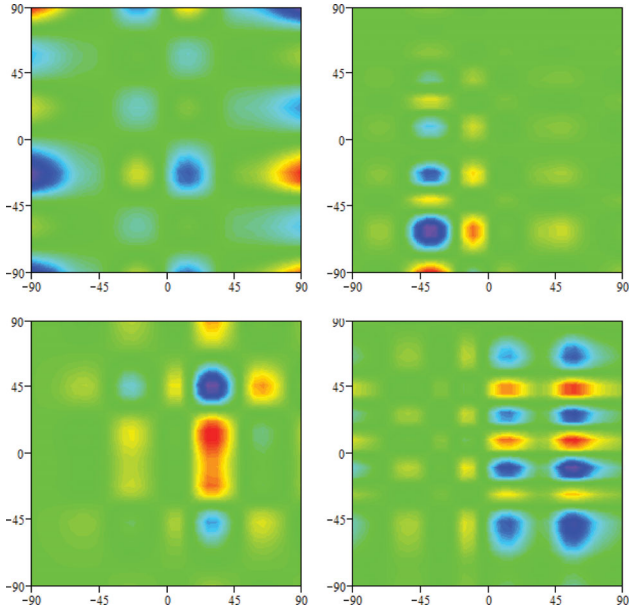

Figure 6. The cross-correlation between the four pairs of EOFs of the SBMF shown in Fig. 5 over the 30 latitude bands corresponding to the common symmetric flows for all three cycles (top left plot) and to cycles 21 (top right plot), 22 (bottom left plot) and 23 (bottom right plot).

eigenvalues as seen in Fig. 1. The next three largest sets of EOFs from Fig. 1 are presented in Fig. 4 for each cycle separately (the second left plots for cycle 21, the third left ones for cycle 22, and the fourth ones, or the rightmost plots, for cycle 23). In Fig. 5 the same waves are presented in different ways to distinguish the variations of their magnitudes: the two main EOFs for all three cycles in the top left plot, EOFs for cycle 21 in the top right plot, EOFs for cycle 22 in the bottom left plot, and EOFs for cycle 23 in the bottom right plot.

It can be noted from these figures that the two main latitudinal EOFs found from the SBMF with the dominant eigenvalues have opposite magnetic polarities and are similar for each solar cycle. At higher latitudes beyond $\pm 40^\circ$, the positive wave is in full anti-phase with the negative one, but at lower latitudes the two waves seem to become coherent and run without any phase shift until they reach latitudes of $\pm 40^\circ$, for the given hemisphere, respectively. In order to achieve this, the positive (negative) magnetic field component passes at about $\pm 40^\circ$ through a wide maximum (minimum) in the Northern hemisphere and through a wide minimum (maximum) in the Southern hemisphere.

Then both waves have their main maxima: in the Southern hemisphere at about -14° for the negative wave and -18° for the positive. Similarly, their minima: in the Northern hemisphere at about 9° for the negative wave and 15° for the positive one. The behaviour of the main negative and positive components follows the patterns of the odd symmetric functions that are likely to correspond to dipole waves from the poles generated by the solar dynamo. In addition, the latitudes of the positive maximum in the Southern hemisphere and the negative minimum in the Northern hemisphere are close to the latitudes approached by the mean sunspot locations found from the butterfly diagram at the end of solar cycle 23 Zharkov & Zharkova (2011).

In the absence of helioseismic data we cannot comment upon $\partial\Omega/\partial\theta$. However, from the data set used in the present paper we can study the derivatives of SBMF variations with latitude ($\partial B/\partial\theta$), which can be considered as a proxy of the derivative $\partial\Omega/\partial\theta$ caused by the latitudinal shear (Benevolenskaya 1998, 2003) discussed in the Introduction. The results of this study are presented in Fig. 7 for the main independent components of the latitudinal variations of the SBMF derived for three cycles from Fig. 5 (top left plot).

The red and blue lines show the derivatives of the EOFs, and the bold magenta line shows their resultant. It can be seen that the SBMF derivatives change significantly over latitude, with the largest change of magnetic flux occurring almost precisely at the equator. This is accompanied by the greatest change in a latitudinal shear decreasing sharply to the latitudes $+30^\circ$ and -20° and then decreasing towards the poles. Keeping in mind that the standard mean dynamo models describe the greatest angular velocity at the equator, decreasing monotonically towards the poles, our results show undoubtedly that the situation is more complex, which needs to be taken into account in future dynamo models.

In addition, there are six other EOFs shown in the next three sets of plots in Fig. 4, corresponding to eigenvalues twice or three times lower in magnitude than the main one. Furthermore, the absolute eigenvalues of EOFs decrease from the top right set in Fig. 4 (corresponding to cycle 21) towards the bottom right set (corresponding to cycle 23), which reflects a decrease of the solar activity index in these cycles.

These six EOFs have paired independent components with either positive or negative waves, which are even functions (with respect to the solar equator) for the odd cycles (21 and 23) and odd functions for the even cycle 22. In cycle 22 the magnitudes of all the maxima

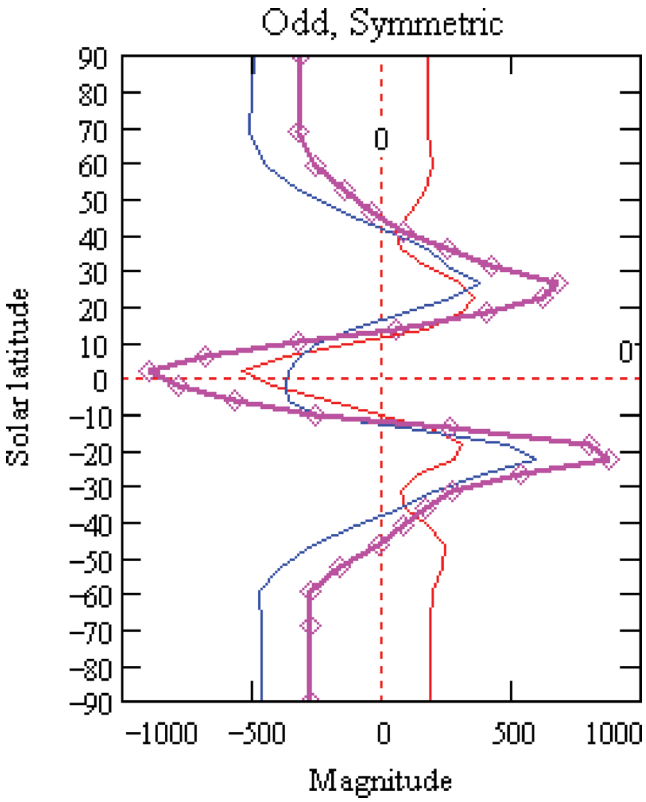

Figure 7. The derivatives of the main EOFs in latitudinal SBMF distribution for cycles 21–23 shown in Fig. 5 (top left plot). The red and blue lines show the derivatives of the components, and the bold magenta line shows their resultant.

and minima are half of the corresponding ones for cycle 21, while the minima and maxima in cycle 23 are also nearly half of those for cycle 22.

In the case of cycle 21 (the second plots from the left) both positive and negative (even) waves have their strongest minima at about 30° (positive) and 20° (negative) in the Northern hemisphere, followed by their maxima at the equator with magnitudes half that of the magnitude of the preceding minima. Furthermore, the maximum of the positive wave is wider than the negative one and has double peaks at each side from the equator.

Then both waves pass through another extremum (maximum for the negative and minimum for the positive wave), with the positive minimum twice that of the negative maximum. In addition, the minimum of the positive wave and the maximum of the negative wave in the Southern hemisphere are half of those in the Northern hemisphere, showing that the waves decay from North to South.

The symmetrically opposite trends are observed for the even cycle 22, revealing from EOFs the decaying waves coming from the South to the North. Both the positive and negative waves become odd functions in cycle 22, passing through zero with respect to the solar equator, so the maxima of the negative wave coincide with the minima of the positive wave. The largest maximum of the negative wave and the minimum of the positive wave occur at latitude 25° in the Southern hemisphere, with the ratio between the magnitudes of the negative-to-positive maxima being around 5.

These extrema are preceded and followed by the maxima for the positive wave or minima for the negative wave: a higher one at latitude $\sim 40^\circ$ and half that for latitude $\sim 8^\circ$. Although the magnitude

of the extrema at the higher latitude is also higher than those at the lower latitude, when the waves move into the Northern hemisphere they have symmetric flat extrema at similar latitudes of about 10°, 20° and 40° in the Southern hemisphere, with the magnitudes of these extrema much lower than the symmetric extrema at the same latitudes in the Southern hemisphere.

For the next odd cycle 23, two, positive and negative, even waves can be observed as in cycle 21, which look nearly symmetric with respect to the equator and fully asymmetric with respect to each other. The fluctuations of the two main EOF components of the SBMF in cycle 23 (the bottom right plot in Fig. 5 and the rightmost two curves in Fig. 4) have their maxima at latitudes 0, +15, −18° and ±40°, with their minima in between. This suggests that in cycle 23 the magnetic field had a three-dipole structure.

The behaviours of the latitudinal EOF distributions of the SBMF are seen much more clearly in the plots showing the cross-correlation between the four EOF pairs in Fig. 6. The top left plot corresponds to the correlation between the two strongest EOFs and shows a very clear quadruple structure, with two dipoles between the poles and a further two located in the equatorial plane. The correlation between the next pair (top right plot) shows a distinct North asymmetry, with the maximum correlation and anti-correlation observed at latitude of ∼65° and the smaller pairs seen at latitude ∼20°, which also indicates a quadruple structure of SBMF.

The correlation of the next pair of EOFs shown in the bottom left plot reveals a South asymmetry, with strong correlation of the components in the pre-equatorial plane (±15°) and similar distinct anti-correlation at latitudes ±45°. The correlation of the last pair shown in the bottom right plot again reveals a North asymmetry, with a chessboard-like structure of the correlation and anti-correlation coefficients occurring in equidistant bands about the equator, supporting the three-dipole structure suggested above from the EOFs themselves.

Hence, the other six EOFs reflect asymmetric and symmetric dynamo waves, which could be produced by a secondary dynamo mechanism, possibly by a turbulent dynamo. The SBMF latitudinal EOFs seem to be strongly related to the temporal PC variations of the SBMF in cycles 21–23 discussed in Section 3.2.

Summarizing the findings above regarding temporal and latitudinal variations of the SBMF (the first two EOFs common to all three cycles and the six secondary EOFs unique for the cycles 21, 22 and 23), one can assume that the main dipole waves produced by the classic dipole solar dynamo mechanism are interacting with various other waves produced by another mechanism defining the meridional flows (turbulent dynamo waves, for example). These EOFs, in addition to dipole waves coming from the poles, could be a reflection of the alternative possibilities of other kind of waves coming from a dipole located at lower latitudes or even at the equator, as suggested by Cadavid et al. (2008). Some of these options will be investigated theoretically in a forthcoming paper.

4 PRINCIPAL COMPONENTS OF THE SUNSPOT MAGNETIC FIELD (SMF) IN CYCLE 23

We can now explore how these dynamo waves detected in the SBMF (assumed to be a poloidal magnetic field) interact with the magnetic field of the sunspots (assumed to be a toroidal magnetic field), which are available from SOHO/MDI in a fully digitized form only for cycle 23.

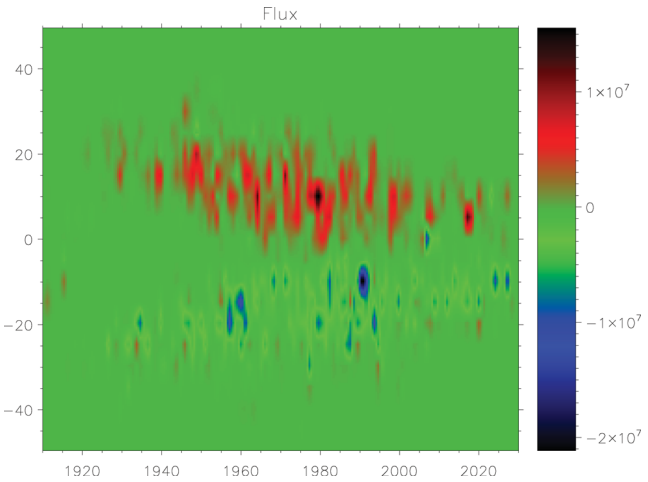

Figure 8. Butterfly diagram for cycle 23 for the daily total SMFs summarized for all the longitudes within narrow latitude strips of 5°. The areas are measured in squared degrees, and the magnetic field in gauss. The CR number 1910 corresponds to the start of 1996, and 2040 to the spring of 2005.

4.1 Quasi-3D butterfly diagram for sunspots

Latitudinal variations of the SMF calculated in narrow latitudinal strips for the whole longitude range in various CRs are presented in Fig. 8. These patterns are similar to the classic Maunder butterfly diagrams for sunspot numbers (Maunder 1904), but with the third dimension associated with the areas covered by sunspots (and thus their magnetic flux) in different latitudinal strips summed for all longitudes (μ-spheres) at different times of the cycle.

During cycle 23 the butterfly diagram for magnetic flux reveals a fine structure in the shape of vertical threads, or strips, changing slightly for every latitude. These strips at any given time interval are brighter (or have larger areas) in one hemisphere than in the other; then, in the next time interval, the strip with larger area shifts to other latitudes or even to the opposite hemisphere. This indicates that there are some periodic oscillations in the appearance of sunspots, which currently define solar activity.

This is confirmed by the auto-correlation of the sunspot excess magnetic flux residuals between the means for 1 yr and 4 yr (1y–4y) in given latitudinal strips, which allowed us to exclude the major anti-symmetric component with period 11 yr, as reported by Zharkov et al. (2008). The auto-correlation of the excess magnetic fluxes in sunspots reveals a well-defined period of ∼2.5 yr, with the negative coefficient confirming the change of sign of this residual. This resembles very closely the phase shift between the two main PCs of the SBMF detected in the present study (see Section 3.2). The physical nature of this latitudinal periodicity is yet to be uncovered, in spite of some previous attempts at interpretation (Benevolenskaya 1998, 2003).

4.2 The PCs of the SMF

Similarly to in the study of the SBMF, a PCA was carried out for the SMF derived from absolute magnetic field magnitudes within the areas covered by sunspots in cycle 23 from the SOHO/MDI data.

As a result, we managed to detect one pair of PCs in the temporal SMF variations plotted in Fig. 9 (the second and fourth plots from the top) and the pair of corresponding EOFs in the latitudinal SMF variations also plotted in Fig. 9 (first and third plots from the top). The first two plots in Fig. 9 present the SMF data used without

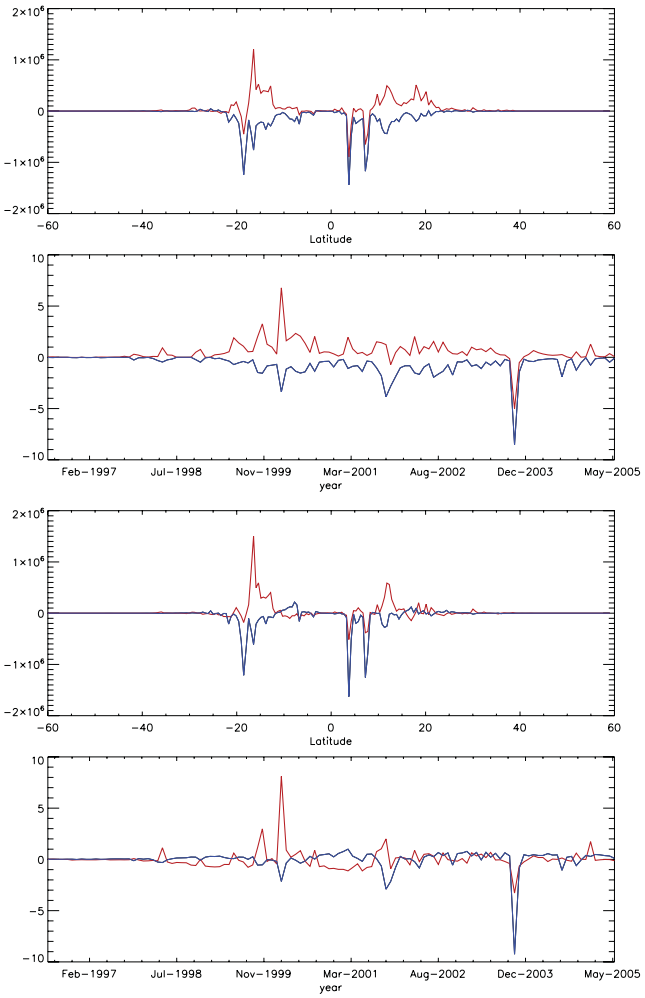

Figure 9. The two PCs of the SMF distribution in time (from the top: second and fourth plots) and EOFs of the SMF distribution in latitude for cycle 23 (from the top: first and third plots) calculated for the raw data (two upper plots) and averaged with the running filter of 39 Carrington rotations (two bottom plots).

any smoothing, and the two bottom plots present the SMF data smoothed over 39 CRs.

It can be noted that, unlike the SBMF, the SMF is found mostly to keep a well-defined parity of its two biggest PCs and EOFs (Fig. 9); for example, each pair of PCs and their EOFs are separated into two components, one positive and one negative. This shows that the derived waves of the magnetic field are separated into opposite hemispheres with a given magnetic field polarity, which is, in fact, the leading magnetic polarity of sunspots for this hemisphere. Further details of their variations are discussed in the sections below.

4.2.1 Latitudinal variations of the SMF

It is evident that the latitudinal EOFs of the SMF have different patterns in the Northern and Southern hemispheres.

First, the EOF with the positive magnetic field polarity (the leading one in the North) has a minimum at -19° and maximum at -17° in the Southern hemisphere, and minima at $+4^\circ$ and $+8^\circ$ and maxima at $+12^\circ$ and $+19^\circ$ in the Northern hemisphere, while the EOF with the negative magnetic field polarity (the leading one in the South) has a minimum at -18° and maxima at -19°, -17° and -15° in the Southern hemisphere, and minima at $+5^\circ$ and $+18^\circ$ and maxima at $+4^\circ$, $+8^\circ$, $+12^\circ$ and $+19^\circ$ in the Northern hemisphere. It turns out that for cycle 23 the latitudes of the last maximum of the positive EOF in the Southern hemisphere and the last minimum of the negative EOF in the Northern one become close to latitudes -14° and $+19^\circ$, which the mean sunspot locations approach at the end of solar cycle 23 (Zharkov & Zharkova 2011).

Second, it can be noted that the sunspot EOFs with opposite polarities are more or less symmetric in the Southern hemisphere, while in the Northern hemisphere they are asymmetric at lower latitudes under 10° and gain symmetry again only at about $+20^\circ$. With the running filter for the data averaging over the 39 CRs (accounting for about 3 yr), the patterns are slightly less clear but are still present. This confirms the strong asymmetry in the sunspot area and magnetic field distributions in the opposite hemispheres reported earlier (Zharkov et al. 2008). This could indicate potentially different routes for toroidal magnetic field propagation in each hemisphere.

If one now compares these patterns in the EOFs for sunspots with the first and last pairs of the EOFs detected for the SBMF in Figs 4 and 5, it can be noted that the positions of the maxima and minima of the positive polarity follow the patterns of the EOFs for the SBMF (sine, marked in blue) shown in the rightmost plot of Fig. 4 and the bottom right plot of Fig. 5, while those of negative polarity follow the patterns of the other EOF (cosine), shown in these figures in red.

This indicates that the latitudinal variations of the solar poloidal magnetic field supposedly defined by the SBMF modulate the latitudinal variations of the toroidal magnetic field defined by the SMF. In the other words, the SBMF seems to regulate the areas of magnetic flux tubes appearing at given latitudes on the solar surface as sunspots. Evidently, during the EOF maxima the magnetic flux tubes have larger areas (and, thus, magnetic field magnitudes) than those occurring during the EOF minima. These magnetic flux tubes are located well beyond the main magnetic poles (North and South), in the 'royal zone', where sunspots are formed by physical processes in addition to the main magnetic dipoles at the poles.

4.2.2 Temporal variations of sunspot PCs

The two PCs in temporal variations of the sunspot magnetic flux plotted in the second plot from the top (for non-smoothed data) and the bottom plot (for data smoothed with a 39-CR filter) shown in Fig. 9 point to a pair of waves with opposite (leading) magnetic polarities travelling in time in opposite hemispheres.

The temporal PCs are found to be nearly symmetric (the maxima in each polarity have similar shapes and magnitudes) in the years from the cycle start up to the cycle maximum. Similarly to the residuals in the PCs in the SBMF (see Fig. 3), the PCs for the SMF reveal two maxima: a smaller one occurred at the start of the year 2000 mainly in the Northern hemisphere, and a larger one occurred at the end of 2003 mainly in the Southern hemisphere. Each period of the maximum PCs in the SMF was accompanied by a number of X-class flares in 2000 and 2003.

The most remarkable pattern is revealed during the autumn of 2003, when the two PCs of the SMF became fully asymmetric (coinciding maximum in the negative PC and minimum in the positive one); the pattern was co-temporal and co-spatial in latitude with the series of Halloween flaring events occurring from the end of October to the end of November 2003. In this period one can observe

very strong oscillations in both temporal PCs derived for the SBMF plotted in Fig. 3, with their maxima and minima coinciding in magnitude and direction, similar to those observed in the PCs of the SMF but having the opposite signs to the SBMF (e.g. a maximum in the SBMF corresponds to a minimum in the SMF and so on).

This suggests that the occurrence of sunspots is strongly modulated by, and is complementary to, the fluctuations of the SBMF not only in latitude but also in time. This modulation is likely to define the asymmetries in sunspot areas and magnetic fluxes derived for cycle 23 (Zharkov et al. 2008).

4.2.3 Sunspot group tilt and charge separation

The latitude distributions of tilt angles presented in Fig. 10 (left-hand plot) for normal sunspot group (GT) tilts reveal the well-known Joy's law (Hale et al. 1919), with a tilt increase from the equator towards higher latitudes, approaching the maximum at latitude 32°. There is a well-known periodic structure in the latitudinal tilt distributions with a period of about 8°; for cycle 23 it shows maxima at 5°, 13°, 20° and 32° followed by a sharp drop of the GT tilts at latitudes higher than 40° (see the top plot in Fig. 10).

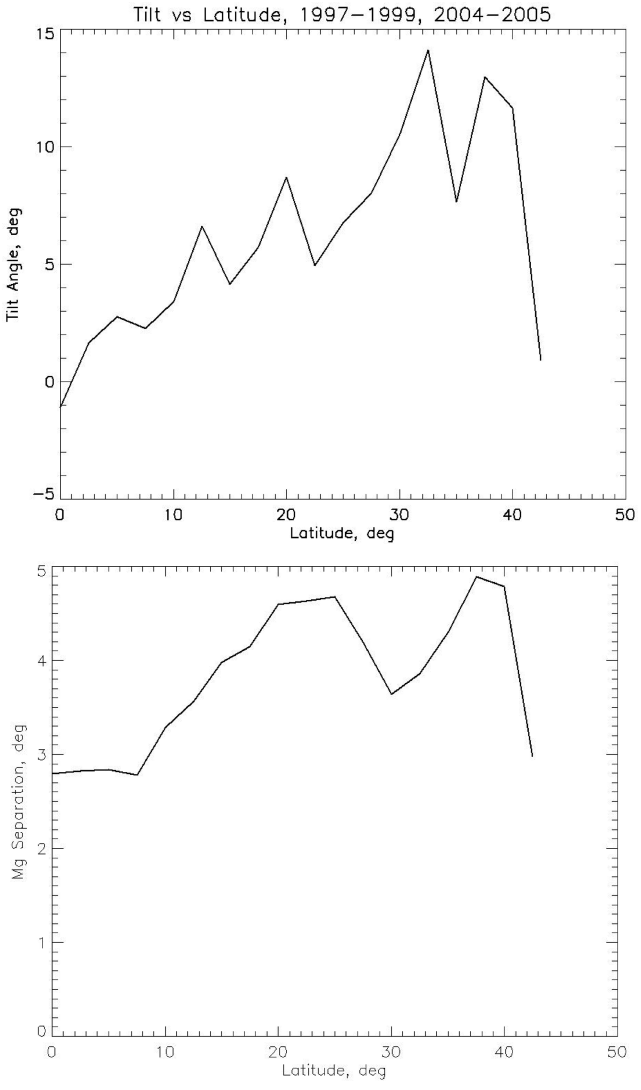

Figure 10. Top plot: the normal tilt distributions versus latitudes for sunspot groups (Joy's law). Bottom plot: the polarity separation versus latitude in sunspot groups in cycle 23.

The magnetic polarity separation in Fig. 10 (bottom plot) also increases from the equator towards the poles, reaching the main maximum of 4.°9 at latitude ∼35°, with the other one of 4.°7 at latitude ∼25°. Similarly, for the tilts themselves the polarity separation sharply decreases after 35° latitude. These maxima in the magnetic polarity separation occur at latitudes where there are minima in the tilt distributions, as noted by Zharkova & Zharkov (2008). Therefore, the changes of magnetic polarity separation are in anti-phase with those in tilts.

Furthermore, it can be seen that the largest EOFs are found in the SMF to be located at latitude positions intermediate to those reported for the maximum of tilts in Joy's law in Fig. 10 (top plot) and to the minimal magnetic polarity separation as in Fig. 10 (bottom plot). This points to higher twists occurring at latitudes with higher tilts, while at latitudes where tilts have minima there are maximal sunspot areas, or magnetic flux, reflected in the occurrence of the maximal PCs in the SMF.

5 DISCUSSION AND CONCLUSIONS

We have derived two temporal PCs in the SBMF with opposite magnetic polarities observed during all three solar cycles 21–23. They are likely to reflect waves that travel off-phase by 90°, or 2.5 yr (shifted like sine and cosine functions), from one hemisphere to another. The wave maxima are achieved in the same hemisphere with a delay of about 2.5 yr, defining (a) the most active hemisphere, and (b) the double maxima of solar activity regularly observed in sunspot occurrence. There are some periods in each cycle when the two waves reach the same magnitude, before and after which there are strong increases in their cyclic residuals that could reflect turbulent processes accompanying the wave interaction in the given hemisphere.

After maxima, the two waves have different temporal patterns: in the odd cycles (21 and 23) the wave with positive polarity (cosine) runs very steeply in the Northern hemisphere towards the equator and then moves smoothly in the Southern hemisphere, while in the even cycle 22 it moves in the opposite direction (from South to the equator and then to the North). The wave with negative polarity (sine) has a much smoother decrease in magnitude, staying in the Northern hemisphere in cycles 21 and 23 (or in the Southern one in cycle 22) until approaching the solar minimum and then moving to the Southern hemisphere in cycle 22 (for the waves in cycle 21).

The magnitudes of maxima of the positive and negative temporal waves steadily decrease by about 50 per cent from cycle 21 to cycle 22 and then by a further 50 per cent to cycle 23, approaching in cycle 23 half of their magnitudes in cycle 21. Furthermore, the magnitude at which these waves intercept, or have the same maxima, is reduced by 30 per cent from cycle 21 to 22 and then by 50 per cent from cycle 22 to cycle 23. For example, in cycle 23, the two waves intercept at the lowest magnitude of about 100, compared with the magnitude of 300 for cycle 21 and of 200 for cycle 22. If the decrease follows the same pattern, then in cycle 24 the waves will intercept at a magnitude of about 50, meaning much lower solar activity compared even to cycle 23.

There are also two main latitudinal components (EOFs) in the SBMF, with dominant eigenvalues that have opposite magnetic polarities and are similar for each solar cycle. At higher latitudes beyond ±40°, the positive wave is in full anti-phase with the negative one, but at lower latitudes they seem to become coherent and run without any phase shift until they reach latitudes of ±40°, for

the given hemisphere, respectively. In order to achieve this, the positive (negative) magnetic field component passes at about $\pm 40^\circ$ through a wide maximum (minimum) in the Northern hemisphere and a wide minimum (maximum) in the Southern hemisphere.

Then both waves have their main maxima: in the Southern hemisphere at about -14° for the negative wave and -18° for the positive wave. Similarly, their minima: in the Northern hemisphere at about 9° for the negative wave and 15° for the positive wave. The behaviour of the main negative and positive components follows the patterns of the odd symmetric functions that is likely to correspond to dipole waves from the poles generated by the solar dynamo. For cycle 23, the latitudes of the positive maximum in the Southern hemisphere and the negative minimum in the Northern one become close to the latitudes approached by the mean sunspot locations at the end of solar cycle 23 (Zharkov & Zharkova 2011).

The derivatives describing the magnetic field shear of the two main EOFs of the SBMF latitudinal variations responsible for the mean dipole dynamo also reveal significant changes of each component of the main EOF pair over latitude, with the maximum occurring almost precisely at the equator, followed by a sharp decrease to latitudes $+30^\circ$ and -20° in the Northern and Southern hemispheres, respectively, and then an increase again towards the poles. This result indicates that the solar dynamo machine does not reveal a monotonic decrease of the latitudinal shear towards the poles assumed by mean dynamo models, and this needs to be taken into account in future simulations.

The periodicities found in the PCs of the SMF show close links with the variations of the PCs of the SBMF, possibly reflecting physical processes affecting the appearance of sunspot groups on the solar surface (rotations, twists induced by propagating dynamo waves, etc.). The temporal PCs of the SMF in cycle 23 from its start to the beginning of decay are found to be slightly asymmetric, with the domination of the Northern polarity, or magnetic flux in the Northern hemisphere. Similarly to the residuals in the SBMF, the PCs for the SMF reveal two maxima: a smaller one occurring at the start and middle in the year 2000, and a larger one occurring at the end of the year 2003, mainly in the Southern hemisphere.

The most remarkable pattern occurred during the autumn of 2003, when the two sunspot PCs become fully asymmetric (a maximum in the negative PC and a minimum in the positive one coincided); this was contemporaneous with the series of Halloween flaring events (the end of October to mid-November 2003). This period was marked in the SBMF by very strong oscillations in both temporal PCs with their maxima coinciding in magnitude and direction, which is opposite to the situation for the PCs in the SMF. This suggests that the occurrence of sunspots is strongly modulated by, and is complementary to, temporal fluctuations of the SBMF.

The variations of the EOFs for the SMF in latitude are also shown to be linked to those of the SBMF. The positions of the maxima and minima of the positive polarity in the EOFs of sunspots follow the patterns of the one of the EOFs (sine), while the sunspot EOFs of negative polarity follow the patterns of the other EOF from the SBMF (cosine). This indicates that the latitudinal variations of the SBMF modulate the latitudinal variations of the SMF. In other words, the SBMF regulates the appearance of magnetic flux tubes on the solar surface, allowing them to have minima at latitudes of $\sim 32^\circ$, 23°, 13° and 3°, where the SBMF (and the sunspot group tilts) has intermediate maxima. The absolute maximum in the tilt magnitudes is approached at the top of the latitudinal zone $\pm 45^\circ$, where SMF EOFs approach zero.

The correlations of the SBMF PCs reveal the presence not of the single dipole assumed for the classic solar dynamo, but of two dipoles in cycles 21 and 22 and, possibly, three dipoles in cycle 23. The presence of the second dipole located at the equator was also suggested by Cadavid et al. (2008) after their PCA of the longitudinal magnetic field variations. However, we established that the additional dipoles occur not only at the equator but also at some latitude bands between 0° and $\pm 40^\circ$ and above $\pm 40^\circ$. We believe that these new findings point out that, in order to account for the appearance of sunspots as current probes of solar activity, one needs to consider in dynamo models not only a dipole but also quadruple or quintuple magnetic sources as the sources of the magnetic waves observed in the Sun.

ACKNOWLEDGMENTS

The authors wish to thank the anonymous referee for constructive and helpful comments, which led to considerable improvements in the paper. VZ and SZ also appreciate the support of this work from the EGSO grant funded by the European Commission in 2002–2005 within Framework 5, and from the Helios grant (SZ) funded by the EC within Framework 7. VZ and SZ also acknowledge current NASA/ESA support of the international FFT network for automated feature detection and classification, which allowed us to contribute to the SDO pipeline with the sunspot and active region detection modules.

REFERENCES

Basu S., Antia H. M., 2006, in Fletcher K., ed., ESA SP-624, Proc. SOHO 18/GONG 2006/HELAS I, Beyond the Spherical Sun. Published on CDROM
Benevolenskaya E. E., 1998, ApJ, 509, L49
Benevolenskaya E. E., 2003, Sol. Phys., 216, 325
Benkhalil A., Zharkova V. V., Zharkov S., Ipson S., 2006, Sol. Phys., 235, 87
Cadavid A. C., Lawrence J. K., McDonald D. P., Ruzmaikin A., 2005a, in Sankarasubramanian K., Penn M., Pevtsov A., eds, ASP Conf. Ser. Vol. 346. Large-scale Structures and their Role in Solar Activity. Astron. Soc. Pac., San Francisco, p. 91
Cadavid A. C., Lawrence J. K., McDonald D. P., Ruzmaikin A., 2005b, Sol. Phys., 226, 359
Cadavid A. C., Lawrence J. K., Ruzmaikin A., 2008, Sol. Phys., 248, 247
Cameron R., Hopkins A., 1998, Sol. Phys., 183, 263
Dikpati M., Gilman P. A., 2008, JA&A, 29, 29
Dikpati M., Gilman P. A., Ulrich R. K., 2010, ApJ, 722, 774
Gizon L., Birch A. C., Spruit H. C., 2010, ARA&A, 48, 289
Gnevyshev M. N., Ol' A. I., 1987, Byulletin Solnechnye Dannye Akademy of Sciences of USSR, No. 1987/8, p. 90
Hale G. E., Ellerman F., Nicholson S. B., Joy A. H., 1919, ApJ, 49, 153
Hathaway D. H., Rightmire L., 2011, ApJ, 729, 80
Hoeksema T., 1984, PhD thesis, Stanford University, CA
Jolliffe I. T., 2002, Principal Component Analysis, 2nd edn. Springer, Berlin
Krause F., Raedler K. H., 1980, Mean-field Magnetohydrodynamics and Dynamo Theory. Pergamon Press, Ltd., Oxford, p. 271
Lawrence J. K., Cadavid A., Ruzmaikin A., 2004, Sol. Phys., 225, 1
Maunder W., Mrs, 1904, MNRAS, 64, 226
Parker E. N., 1955, ApJ, 122, 293
Pearson K., 1901, Phil. Mag., 2, 559
Scherrer P. H., Wilcox J. M., Kotov V., Severnyi A. B., Howard R., 1977, Sol. Phys., 52, 3
Schlichenmaier R., Stix M., 1995, A&A, 302, 264
Schou J. et al., 1998, ApJ, 505, 390
Snodgrass H. B., Dailey S. B., 1996, Sol. Phys., 163, 21

Steenbeck M., Krause F., Rädler K.-H., 1966, Zeitschrift Naturforschung Teil A, 21, 369
Švanda M., Klvaňa M., Sobotka M., 2006, A&A, 458, 301
Ulrich R. K., 1993, in Weiss W. W., Baglin A., eds, ASP Conf. Ser., Vol. 40, IAU Colloq. 137, Inside the Stars. Astron. Soc. Pac., San Francisco, p. 25
Zharkov S. I., Zharkova V. V., 2011, J. Atmospheric Solar-Terrestrial Phys., 73, 264
Zharkov S., Zharkova V. V., Ipson S. S., 2005, Sol. Phys., 228, 377
Zharkov S., Gavryuseva E., Zharkova V., 2008, Sol. Phys., 248, 339
Zharkova V. V., Zharkov S. I., 2008, Adv. Space Res., 41, 881
Zharkova V. V., Zharkov S. I., 2010, Adv. Geosci., 21, 289
Zharkova V. V., Aboudarham J., Zharkov S., Ipson S. S., Benkhalil A. K., Fuller N., 2005, Sol. Phys., 228, 361

This paper has been typeset from a TEX/LATEX file prepared by the author.